A system for optically controlling neural circuits with very high spatial and temporal resolution

Chethan Pandarinath, Eric T. Carlson, and Sheila Nirenberg

Abstract — **Optogenetics offers a powerful new approach for controlling neural circuits. It has a vast array of applications in both basic and clinical science. For basic science, it opens the door to unraveling circuit operations, since one can perturb specific circuit components with high spatial (single cell) and high temporal (millisecond) resolution. For clinical applications, it allows new kinds of selective treatments, because it provides a method to inactivate or activate specific components in a malfunctioning circuit and bring it back into a normal operating range [1-3]. To harness the power of optogenetics, though, one needs stimulating tools that work with the same high spatial and temporal resolution as the molecules themselves, the channelrhodopsins. To date, most stimulating tools require a tradeoff between spatial and temporal precision and are prohibitively expensive to integrate into a stimulating/recording setup in a laboratory or a device in a clinical setting [4, 5]. Here we describe a Digital Light Processing (DLP)-based system capable of extremely high temporal resolution (sub-millisecond), without sacrificing spatial resolution. Furthermore, it is constructed using off-the-shelf components, making it feasible for a broad range of biology and bioengineering labs. Using transgenic mice that express channelrhodopsin-2 (ChR2), we demonstrate the system's capability for stimulating channelrhodopsin-expressing neurons in tissue with single cell and sub-millisecond precision.**

I. Introduction

A limitation for the use of optogenetic technology is driving the optogenetic protein, such as a channelrhodopsin or halorhodopsin, with precise spatial and temporal resolution. Because these proteins require bright light, standard devices that provide high resolution, such as CRT or LCD monitors, are not effective: the light level is orders of magnitude lower than the 0.1-10mW/mm^2 typically needed (reviewed in [4]; see also [2, 5-9]). For example, with ChR2 driven by an array of promoters including CAMKII, Chicken beta-actin, and Thy-1 [2, 4, 10], the light intensity needed to produce precise temporal resolution (1 spike per pulse) was at least 0.5 mW/mm^2, and about 0.1 mW/mm^2 to produce responses at all [6]. Devices such as LEDs and lasers can meet this light-intensity need, but aren't readily suitable for providing spatially-patterned stimuli [10, 11].

Manuscript received July 30, 2013. This work was funded by National Institutes of Health grant EY012978, and the BioAccelerate NYC Prize from the New York City Economic Development Corporation.

C.P., E.T.C., and S.N. are with the Department of Physiology and Biophysics, Weill Medical College of Cornell University, New York, NY 10065. (Correspondence to S.N.: shn2010@med.cornell.edu).

Present address for C.P.: Department of Electrical Engineering, Stanford University, Stanford, CA.

To address this problem, several groups have been developing new devices, each approaching the problem from a different angle. For example, Grossman et al. [4] used a Light-emitting Diode (LED) approach based on a fabrication of a two-dimensional high power micro-LED array (MLA); this device can generate arbitrary excitation patterns with micron and sub-millisecond resolutions and sufficient irradiance to generate ChR2-evoked spiking in neurons. This offers a potential solution in the long-term. However, at present, the limited number of pixels (64x64), fixed wavelength, and the cost and complexity of fabrication, limits its use for wide translation to biology laboratories. Strategies built around Digital Micro-mirror Devices (DMDs) have also been developed. Applications have been targeted largely toward research in *Caenorhabditis elegans* (*C. elegans*) [5, 7]. In particular, Leifer et al. [5] advanced the method to study freely-moving *C. elegans* and achieved a combined stimulating/recording system that operates with reasonably high spatial resolution (30 μm). The DMD device they used (TI DLP Discovery 4000) itself is fast, but the whole system - camera, DMD, image processing software - together slows it down (to ~ 50 frames per second). It met their needs, but it doesn't generalize to those of biology labs in general and is prohibitively expensive. DMD stimulators have been used in other applications as well [12], but the temporal resolution has been slow relative to the resolution needed to stimulate cells with biological neural codes.

Here, we present an inexpensive (< $1000) system with both very high spatial and temporal resolution (< 8 μm spatial and < 1 ms temporal). Thus, it provides a method that is affordable across the board to biology labs, and achieves the resolution needed for both basic science and clinical purposes – spatial resolution at the level (or finer) of single cells, and temporal resolution at the level (or finer) of single action potentials.

II. Methods

The stimulation device contains two subsystems: a control system and a modified mini-digital light processor (mDLP). The control component consists of a single-board computer that controls the display of stimuli on the mDLP. The mDLP was designed around the Pico Projector Development Kit v2.0 (Texas Instruments, Dallas, TX). This kit has three main components: a digital micromirror device (DMD) and its control circuitry, the output lens module, and the light module. Two of these, the light module and output lens module, were replaced with custom components as

978-1-4799-3163-7/13/$31.00 ©2013 IEEE

described in detail below.

A. Control System

The control system was a low-cost, single-board computer (Beagleboard rev. C4, Texas Instruments, Dallas, TX). The computer is powered by a 720MHz ARM Cortex A8 processor, which provides ample processing power to perform high-speed stimulus presentation with minimal jitter. The computer connects to the mDLP via an HDMI connection, which sends both display data and control signals to the mDLP. Users connect to the control system over ethernet using a USB 2.0 network interface (ZUN2210, Zonet USA, City of Industry, CA). Stimuli were presented on the display using custom software written in C.

B. Digital Micromirror Device

The DMD contained in the Pico Projector Development kit is a 0.17" HVGA chip (DLP1700, Texas Instruments). It consists of a 480 x 320 array of micromirrors, each 7.6 μm x 7.6 μm. The development kit also includes control circuitry to receive input images over an HDMI connection and present them on the DMD. Importantly, the control circuitry included in the development kit allows access to high-speed presentation modes – in the highest speed monochrome mode, each pixel on the DMD can be individually switched on or off at up to 1440 Hz.

C. Output lens module

The Pico Projector Development kit includes a projector lens intended for projecting images onto large areas (e.g. for presentations). To produce a smaller image that would provide the intensity and spatial resolution needed to drive ChR2 for neuroscience needs, as well as 1:1 imaging, two Steinheil Triplet Achromatic lenses were added (9 mm diameter and 18 mm effective focal length (NT45-399, Edmund Optics, Barrington, NJ)). A lens holder was made to secure the lenses using two pieces of brass tubing: an outer tube that surrounded the lenses, and an inner tube that held them securely in place (outer: 13/32" OD, 8859K29, inner: 3/8" OD, 8859K28, McMaster-Carr, Santa Fe Springs, CA). The inside of the holder was coated with black paint mixed with grit to produce a dark, rough-textured wall that reduced reflections. To minimize stray light, a 4 mm diameter aperture was created using black aluminum foil and placed between the DMD and the first lens.

D. Light module

The light module consists of LEDs (which act as the light source for the mDLP) and lenses to diffuse the output of the LEDs in order to illuminate the DMD more uniformly. The RGB LED set that comes with the Pico Kit was replaced with a high-powered LED (XP-E Blue, Cree Inc., Durham, NC). This LED has a peak output wavelength of 475 nm and a narrow emission profile (illustrated in Fig. 1(a)). To dissipate heat, the LED was attached to a 45 mm x 45 mm heat sink using conductive thermal epoxy, allowing the LED to be run at continuously high intensities (up to 1 A current). This enabled high output intensities (> 2.5 mW/mm^2) when using a 1:1 imaging configuration (see Fig. 1(c)). The output intensity of the LED was precisely controlled using a variable power supply (HQ Power PS 3003U, Velleman, Ft. Worth, TX). For fixed intensities, stable performance was also readily achieved using a voltage-controlled current source (LuxDrive BuckPuck 3023, Randolph, VT). Light intensity (absolute power) measurements were taken using a New Focus 3803 Power Meter (San Jose, CA). Measurements requiring precise timing used a silicon photodiode with a 20 ns rise time (BPW 34, OSRAM, Munich, Germany) and sampled at 40 kHz using a NI USB-6009 DAQ (National Instruments, Austin, TX).

E. Transgenic animals

Retinas from a transgenic mouse line that expresses ChR2 in the ganglion cells were used to test the device (n=15). In this mouse line, the promoter for the Thy1 gene drives expression of a construct consisting of the ChR2 gene fused to the gene for Yellow Fluorescent Protein (ChR2-YFP). This Thy1-ChR2-YFP line was obtained from Jackson Labs (B6.Cg-Tg(Thy1-COP4/EYFP)9Gfng/J; stock number 007615). For controls, the device was tested on retinas from mice from the same strain that did not express Channelrhodopsin (i.e., non-expressing siblings), and, additionally, on retinas from an rd1/rd1 mouse line (C3H/HeN, Charles River), a standard blind mouse line that also does not express Channelrhodopsin (see ref. [2]). As shown in ref. [2], Fig. 2e, control retinas show no patterned firing in response to stimulation, only spontaneous activity.

F. Multielectrode Recording/Pharmacology

Device performance was assessed using extracellular recordings from the ChR2-expressing retinal ganglion cells of the Thy1-ChR2-YFP mice, following [2]. Spike trains were recorded and sorted into single units using a Plexon Multichannel Acquisition Processor (Dallas, TX, USA).

Because the retina contains intrinsic light-sensitive cells (photoreceptors), neurotransmitter blockers were used to ensure that light-driven responses were due to stimulation of the ChR2 in the ganglion cells and not stimulation of the photoreceptors, as in [2, 13]. The following were used: 10 μM CPP ((±)-3-(2-Carboxypiperazin-4-yl) propyl-1-phosphonic acid), 10 μM NBQX (1,2,3,4-Tetrahydro-6-nitro-2,3-dioxo-benzo[f]quinoxaline-7-sulfonamide), which block NMDA and AMPA/kainate receptors, respectively, and 80 μM APB (2-amino-4-phosphonobutyrate), which blocks metabotropic glutamate receptors.

III. Results

To create a system that can precisely stimulate optogenetic proteins, three factors are critical: high light intensities, high temporal resolution, and the ability to produce patterned stimuli with high spatial resolution.

A. Generating high light intensities

As is well-known, the light intensity needed to drive

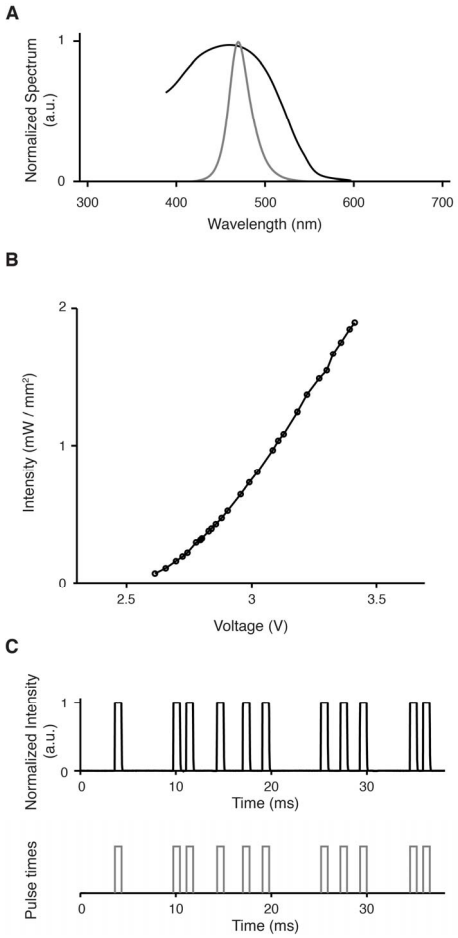

Fig. 1. Spectral, irradiance, and temporal characteristics of the stimulation device are optimized for precise stimulation of channelrhodopsin, in this case, ChR2. (a) Spectral characteristics of the stimulator's LED allow efficient stimulation of ChR2. Normalized emission spectrum of the LED (*grey*) superimposed on the ChR2 action spectrum (*black*, estimated from Nagel et al. [14]). Note that simply replacing the blue LED in the stimulator with an LED that has a different emission spectrum allows activation of channelrhodopsins with other absorption spectra. (b) Intensity vs. Voltage for 1:1 imaging configuration (1 μm on the micromirror array equals 1 μm on the projected image). Previous work has demonstrated that precise spike timing with ChR2 requires light intensities > 0.5 mW/mm^2 [2]. The system's output clearly covers this range. (See Fig. 4 for spiking output as a function of intensity.) (c) The system's output is able to transition between on and off states with sub-millisecond resolution (0.7 ms), allowing it to tightly follow the signals it receives. *Black* shows the pattern of light pulses produced by the device; *grey* shows the underlying pattern of electronic pulses sent from the device's software.

ChR2 varies with wavelength; this is shown in the ChR2 action spectrum (Fig. 1(a), black trace). Maximum absorption occurs at ~460 nm. To stimulate ChR2 with high efficiency, we chose as our light source a high-powered LED whose peak emission (475 nm) is very close to the maximum absorption of ChR2 (Fig. 1(a), grey trace).

Previous work by several groups has demonstrated that high light intensities are needed to elicit action potentials from ChR2-expressing neurons – at least 0.1 mW/mm^2 to drive ChR2 at all, and at least 0.5 mW/mm^2 to produce precise temporal resolution [2, 4, 6, 10]. To determine whether our system's output was capable of reaching these intensities, we measured the irradiance (power / unit area) of the system's output as a function of LED input voltage. The results demonstrate that the system achieves the desired output intensities, with a peak output above 1.75 mW/mm^2. Output was measured using a 1:1 imaging configuration (1 μm on the micromirror array equals 1 μm on the projected image); a fixed-size stimulus was projected onto a power meter, and irradiance measurements were taken as the input voltage to the device's LED was varied. As shown (Fig. 1(b)), the input voltage was varied between 2.6 V to 3.4 V, which produced a range of irradiance between 0.07 mW/mm^2 to 1.90 mW/mm^2. This range was well above what was needed for precise stimulation of ChR2 (e.g., ~3 times greater than the intensity that was needed for ms precision in [2]). At the highest voltage used here, the current through the LED was 0.76 A.

B. Producing high temporal resolution

Next we tested whether the system's output was capable of generating light pulses with precise temporal resolution. Fig. 1(c) shows the normalized output intensity during presentation of a pre-set sequence of light pulses, as measured using a photodiode. The width of each pulse was 0.7 ms, the minimum allowed by the 1440 Hz switching speed of the digital micromirror device (DMD). The DMD is an array of micromirrors whose state (on position or off position) determines the output intensity at a given pixel. As transitions between on and off states are governed by the switching speed of the mirrors, the system's output is able to transition between these states with sub-millisecond precision, allowing very sharp temporal transitions.

C. Producing patterned stimuli with high spatial resolution

The third critical factor in precisely driving channelrhodopsins is the ability to produce spatially patterned stimuli with high resolution. In the case of our mDLP device, the spatial resolution is set by the spatial characteristics of the DMD. One distinct advantage of DMD technology over other array technology is that the mirrors on the DMD are tightly packed together (illustrated schematically in Fig. 2(a), *left*). The tight packing (low inter-mirror spacing) allows nearly the entire area to be illuminated without gaps or "dead spots". This packing is quantified by the fill factor: the fraction of the total area that is illuminated. The fill factor for the DMD-based stimulation system is >80%, more than a factor of 5 better than displays based on micro-LED arrays, which have fill factors of ~16% (e.g. Fig. 2(a), *right*, estimated from Grossman et al. [4]).

To characterize the spatial properties of the system's output, we acquired images of the output by focusing it onto a CCD camera, using the custom output lens module. The output lens module consists of two 18 mm focal length Steinheil Triplet Lenses, configured in a 4 *f* relay configuration, which provides 1:1 imaging (1 μm on the CCD sensor equals 1 μm on the DMD). Fig. 2(b) shows the spatial characteristics with all pixels illuminated,

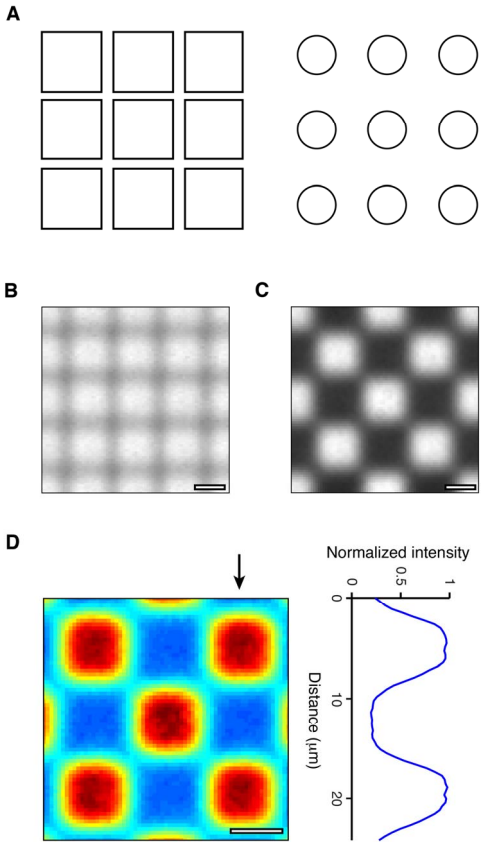

Fig. 2. Spatial characteristics of the Digital Micromirror Device (DMD). (a) *Left,* schematic illustrating the high fill factor (i.e., fine inter-pixel spacing) of the DMD. *Right*, schematic illustrating the spacing of pixels in a comparable device, the micro-LED array (estimated from [4]). (b) DMD Image output with all pixels illuminated (i.e., all mirrors in the "on" position). The center-to-center spacing between pixels is 7.6 μm in the horizontal and vertical directions. (c) DMD image from the same configuration, but with a spatially patterned output (checkerboard). (d). *Left*, image in *(c)* expanded and plotted as an intensity map. Arrow indicates column plotted as an intensity profile (*right*). Scale bar = 5 μm (*b*, *c*, *d*).

demonstrating the high fill factor of the final projected output. The center-to-center spacing of the pixels on the array is 7.6 μm in the horizontal and vertical directions. Fig. 2(c) shows an example of the device's output when presenting a patterned stimulus, in this case, a checkerboard. This output is expanded and plotted as an intensity map in Fig. 2(d). The mean full width at half maximum (FWHM) of the pixels was 6.90 +/- 0.04 μm (mean +/- SEM), indicating that each pixel produces a sharp spot with low bleed between neighboring pixels.

D. Effectiveness of the stimulation system for stimulating ChR2 in tissue

The results of the characterization experiments show that the device has favorable temporal, spatial, and output light intensity properties for stimulating ChR2. Next we demonstrated its effectiveness for stimulating ChR2-expressing neurons in actual tissue, using the excised retina as the model system. The device stimulates the ChR2-expressing neurons in the tissue while the firing patterns of the ChR2 cells are recorded extracellularly using a 64

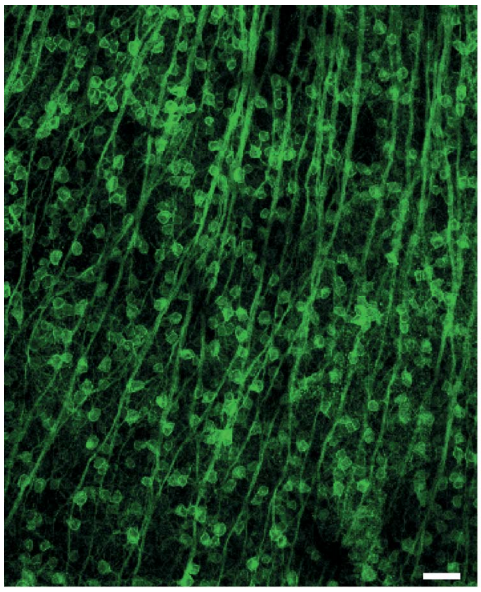

Fig 3. Channelrhodopsin-expressing cells in neural tissue. The tissue is mouse retina; the ChR2-expressing cells are the retinal ganglion cells; scale bar = 50 μm (image adapted from [2]). Note the high-density of the ChR2-expressing cells; approximately 1/3 of the cells in the population express the protein. This illustrates the need for a device capable of high density, multisite stimulation.

channel multi-electrode array. The custom output lens module in the 1:1 imaging configuration allows the device's output to be focused onto the ChR2-expressing cells without external lenses. Fig. 3 shows the tissue used to test the device, excised retina from a transgenic mouse line that expresses ChR2 under control of the Thy-1 promoter. We chose this tissue because the density of the ChR2-expressing cells is high (approximately 1/3 of the cells in the population express it), emphasizing the need for devices capable of high density, multisite stimulation with independently-controlled stimulators.

In Fig. 4, we show that the device, which is capable of producing light pulses with fine temporal resolution (Fig. 1(c)), can correspondingly produce spikes in the tissue with fine temporal resolution. A series of raster plots is shown that vary in the intensity used to drive the ChR2 (from 0.1 to 1 mW/mm^2). In each, the stimulation was a brief (1.4 ms) pulse of light, and the spikes produced by the ChR2-expressing retinal ganglion cells were recorded. The tightest coupling between the light pulses and the spikes was elicited at an intermediate intensity (0.6 mW/mm^2). Fig. 4(b) shows the relationship between light intensity and spike number, and Fig. 4(c) shows the relationship between light intensity and latency. These results demonstrate that the intensity range produced by the device covers the range needed to elicit spikes with precise temporal resolution.

Finally, we show the performance of the device in the spatial domain. Fig. 2 showed that the device has spatial resolution to allow many cells in a tissue to be stimulated simultaneously; in Fig. 5, we demonstrate this in tissue, again using the retina as the model system. The procedure used for stimulating the cells and for mapping their locations

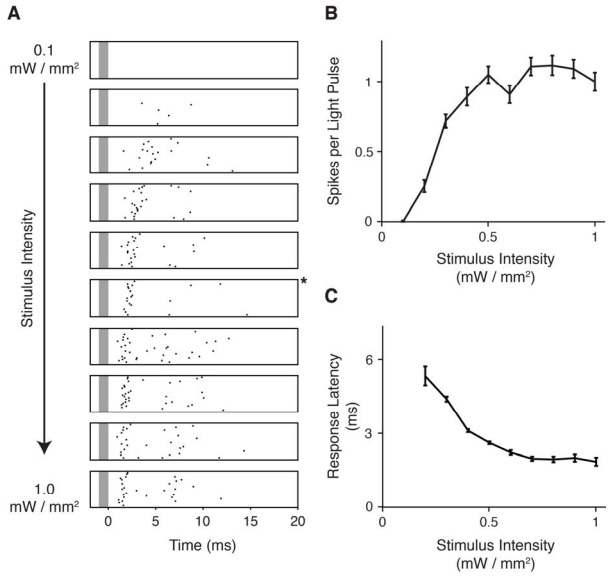

Fig. 4. **The device generates the intensities needed for precise stimulation.** (a) Responses to light pulses over a range of stimulus intensities (0.1 mW/mm^2 to 1 mW/mm^2). Stimuli were 1.4 ms pulses of light, each spaced 100 ms apart. *Grey bar* indicates the time of the light pulse. *Black dots* indicate the time of a single spike, and each row represents a different trial. 25 trials are shown for each intensity. Star denotes an intermediate intensity, 0.6 mW/mm^2, in which very tight coupling between light pulses and spiking activity was achieved, consistent with [2], where 0.7 mW/mm^2 was used to drive reliable precise spiking with ChR2. (b) Number of spikes elicited by each light pulse as a function of stimulus intensity (mean +/- SEM). (c) Response latency as a function of stimulus intensity (mean +/- SEM). Higher intensities elicited faster responses, with latencies as short as 2-3 ms for 1 mW/mm^2.

in the retina is shown in Fig. 5(a): We presented a random checkerboard stimulus with checkers of 38 μm x 38 μm (size chosen to sufficiently stimulate retinal ganglion cells, whose cell bodies range from 10 – 25 μm). Each checker was turned on or off randomly in time, and action potentials (spikes) were recorded from the retina's ganglion cells. The location of each ChR2-expressing cell was then determined by reverse correlating the spikes from the cells to the checkerboard patterns. For each cell, the average checkerboard that preceded its spikes was then computed. Fig. 5(b) shows the results for ten cells. The peak of the average checkerboard is shown for each. These results show that with this device, many cells can be stimulated independently, as is essential for many purposes in both basic and applied science.

IV. Discussion

In this paper we present a system capable for stimulating optogenetic targets that has precise temporal and spatial stimulation and can be constructed in a cost-effective manner using off-the-shelf components. Such as system is critical for many purposes in both basic science (for studying population coding) and for clinical applications (for building optogenetic prosthetic devices).

We demonstrated the effectiveness of the device by simultaneously stimulating many individual ChR2-expressing cells in the excised retina. For this test case, we used a configuration that allowed a large area to be targeted (roughly 3.6 mm x 2.4 mm). This configuration was based on a 1:1 magnification ratio, but the system can readily be adapted for other requirements. E.g., a smaller magnification ratio could be used to target larger areas. While this would necessarily lower the output intensity (by spreading light over a larger area), the LED's output current can be adjusted to increase the overall power output, as demonstrated in Fig. 1; thus, the system's design allows a 2-3 times larger area to be illuminated while maintaining the 0.5 - 1 mW/mm^2 intensity range needed to precisely drive ChR2. Conversely, a larger magnification ratio could be used to target a smaller area. This would reduce the size of each pixel (from the 7.6 μm x 7.6 μm per pixel in our configuration), allowing the experimenter to probe neural circuitry at an even finer spatial resolution.

We demonstrated the system's effectiveness using a first generation channelrhodopsin, ChR2. Our device can also be paired with the newer optogenetic compounds [15, 16], including ones that allow action potentials to be elicited at high rates (~200 Hz), as the device provides sub-millisecond precision. Further, because of the flexibility in the input light path, one can drive multiple light-sensitive opsins by multiplexing multiple light sources. For example, experimental setups that pair excitatory and inhibitory opsins allow for selective excitation and inhibition (e.g. ChR2 and Halorhodopsin, as in Han and Boyden [17] and Greenberg et al. [18]). To stimulate these opsins in parallel, multiple light sources would be required (such as a blue source for ChR2, and a yellow source for Halorhodopsin). These light sources could readily be integrated into the mDLP's input light path using a dichroic beam combiner, and stimulation patterns specific to each opsin could be presented through time-multiplexing (e.g., for the ChR2/Halorhodopsin example, one would alternately illuminate the blue and yellow light sources, allowing the blue- and yellow-sensitive targets to be driven in alternate frames) [19].

One technology that provides a similar functional output to our system is the micro-LED array [4]. This device centers on a custom-fabricated array of LEDs, each of which is individually addressable. Though the micro-LED array produces similar output to the DLP-based approach, there are some important differentiating factors: A major advantage of the DLP approach is that the fill factor is more than 5 times greater, as shown in Fig. 2. This is because the inter-mirror spacing of the DMD is quite low; in the LED case, the minimum inter-LED spacing is restricted by the bonding process between the LEDs and the interconnects necessary to drive them. This limits the minimum inter-LED spacing to 50-100 μm [4, 20]. A proposed solution to the fill factor issue is the integration of a micro-lens array over the LEDs [4] – this would effectively fill the "dead spots" between LEDs by spreading out the light from each LED. However, this would also decrease the power output by the LEDs (by spreading the light over a larger area). For example, a lens-array that spread each LED's output by a

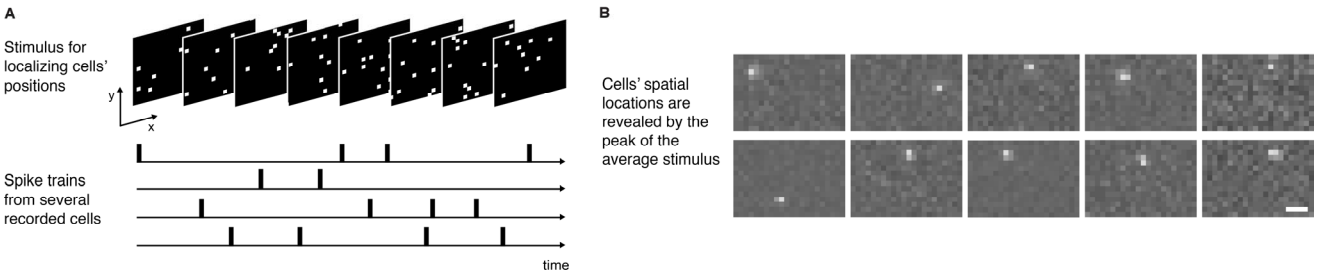

Fig. 5. Simultaneous targeting of many cells in a tissue; the locations of ten cells are shown. (a) A reverse correlation procedure was used for finding the spatial locations of the ChR2-expressing cells in a tissue. The stimulus used was a checkerboard whose checkers were turned either on or off at random every 1.4 ms. The responses (spike trains) of the cells were recorded using a multielectrode array. The location of each ChR2-expressing cell was then determined by reverse correlating the spikes to the stimuli that preceded them. The average stimulus was then computed. (b) Results of this procedure performed simultaneously for ten cells. The peak of the average stimulus for each cell is shown. Scale bar = 150 μm.

factor of 4 would also decrease the effective stimulation intensity by the same factor. A second drawback of the micro-LED based approach is that current LED-addressing hardware limits the addressing speed (and therefore temporal resolution) of the system to approximately 40 Hz [4], compared to the 1440Hz achievable with the DLP approach. This may eventually be solved through the development and integration of a custom CMOS control chip to allow the LEDs to be addressed more quickly [21]. However, at present, the limited temporal resolution is a significant barrier to the utility of the micro-LED technology. Furthermore, there are many applications in the basic science and clinical realms that may benefit from the ability to stimulate using multiple wavelengths of light. As noted earlier, the DLP-based approach provides a very flexible input light path, which allows the easy integration of multiple light sources. Currently, it is unclear how one might integrate multiple wavelengths with the micro-LED approach.

A potential criticism of the DLP approach is that power requirements are greater than those of micro-LED arrays, as the DLP requires all pixels to be illuminated at all times, regardless of their state (on or off). In contrast, LED matrices only require power proportional to the number of pixels that are illuminated, and therefore save energy. This could be advantageous in a mobile system, such as a retinal prosthetic application. However, the power requirements to drive the LED are not large. For example, in Fig. 4, the configuration that produced the tightest coupling between light pulses and spikes was 0.6 mW/mm^2. To produce this intensity, the LED required ~ 0.5 W; this is approximately half the power required when making a call with a typical cellular phone [22]. Thus, the power requirements of the DLP-based approach do not critically limit the implementation of a prosthetic system.

REFERENCES

[1] V. Gradinaru, *et al.*, "Optical deconstruction of parkinsonian neural circuitry," *Science,* vol. 324, pp. 354-9, Apr 17 2009.

[2] S. Nirenberg and C. Pandarinath, "Retinal prosthetic strategy with the capacity to restore normal vision," *Proc Natl Acad Sci U S A,* vol. 109, pp. 15012-7, Sep 11 2012.

[3] J. T. Paz, *et al.*, "Closed-loop optogenetic control of thalamus as a tool for interrupting seizures after cortical injury," *Nat Neurosci,* vol. 16, pp. 64-70, Jan 2013.

[4] N. Grossman, *et al.*, "Multi-site optical excitation using ChR2 and micro-LED array," *J Neural Eng,* vol. 7, p. 16004, Feb 2010.

[5] A. M. Leifer, *et al.*, "Optogenetic manipulation of neural activity in freely moving Caenorhabditis elegans," *Nat Methods,* vol. 8, pp. 147-52, Feb 2011.

[6] H. Wang, *et al.*, "High-speed mapping of synaptic connectivity using photostimulation in Channelrhodopsin-2 transgenic mice," *Proc Natl Acad Sci U S A,* vol. 104, pp. 8143-8, May 8 2007.

[7] Z. V. Guo, *et al.*, "Optical interrogation of neural circuits in Caenorhabditis elegans," *Nat Methods,* vol. 6, pp. 891-6, Dec 2009.

[8] J. P. Weick, *et al.*, "Functional control of transplantable human ESC-derived neurons via optogenetic targeting," *Stem Cells,* vol. 28, pp. 2008-16, Nov 2010.

[9] J. N. Stirman, *et al.*, "Real-time multimodal optical control of neurons and muscles in freely behaving Caenorhabditis elegans," *Nat Methods,* vol. 8, pp. 153-8, Feb 2011.

[10] A. M. Aravanis, *et al.*, "An optical neural interface: in vivo control of rodent motor cortex with integrated fiberoptic and optogenetic technology," *J Neural Eng,* vol. 4, pp. S143-56, Sep 2007.

[11] L. Campagnola, *et al.*, "Fiber-coupled light-emitting diode for localized photostimulation of neurons expressing channelrhodopsin-2," *J Neurosci Methods,* vol. 169, pp. 27-33, Mar 30 2008.

[12] N. Farah, *et al.*, "Patterned optical activation of retinal ganglion cells," in *Proc IEEE EMBS*, Lyon, France, 2007, pp. 6368-70.

[13] P. S. Lagali, *et al.*, "Light-activated channels targeted to ON bipolar cells restore visual function in retinal degeneration," *Nat Neurosci,* vol. 11, pp. 667-75, Jun 2008.

[14] G. Nagel, *et al.*, "Channelrhodopsin-2, a directly light-gated cation-selective membrane channel," *Proc Natl Acad Sci U S A,* vol. 100, pp. 13940-5, Nov 25 2003.

[15] J. Y. Lin, *et al.*, "Characterization of engineered channelrhodopsin variants with improved properties and kinetics," *Biophys J,* vol. 96, pp. 1803-14, Mar 4 2009.

[16] L. A. Gunaydin, *et al.*, "Ultrafast optogenetic control," *Nat Neurosci,* vol. 13, pp. 387-92, Mar 2010.

[17] X. Han and E. S. Boyden, "Multiple-color optical activation, silencing, and desynchronization of neural activity, with single-spike temporal resolution," *PLoS One,* vol. 2, p. e299, 2007.

[18] K. P. Greenberg, *et al.*, "Differential targeting of optical neuromodulators to ganglion cell soma and dendrites allows dynamic control of center-surround antagonism," *Neuron,* vol. 69, pp. 713-20, Feb 24 2011.

[19] S. Nirenberg, *et al.*, "Retina Prosthesis. International Patent WO2012030625," 2012.

[20] P. Degenaar, *et al.*, "Optobionic vision--a new genetically enhanced light on retinal prosthesis," *J Neural Eng,* vol. 6, p. 035007, Jun 2009.

[21] B. R. Rae, *et al.*, "CMOS driven micro-pixel LEDs integrated with single photon avalanche diodes for time resolved fluorescence measurements," *Journal of Physics D: Applied Physics,* vol. 41, p. 094011, May 04 2008.

[22] A. Carroll and G. Heiser, "An analysis of power consumption in a smartphone," in *Proc USENIX Ann Tech Conf*, Boston, MA, 2010, pp. 271-284.